


Alternate-Day High Fat-Normal Chow Diet Ameliorates HFD-Induced Obesity and Restores Intestinal Immunity

Drake Z Ao¹, Yihua Xu², Xueting Sun², Weibo Zhang¹, Ye Yuan²

¹The Affiliated High School of Peking University, Beijing, 100086, People's Republic of China; ²Institute of Molecular Medicine, College of Future Technology, Peking University, Beijing, 100871, People's Republic of China

Correspondence: Ye Yuan, Institute of Molecular Medicine, College of Future Technology, Peking University, Beijing, 100871, People's Republic of China, Email yuaneyy@pku.edu.cn; Weibo Zhang, The Affiliated High School of Peking University, Beijing, 100086, People's Republic of China, Email zhangweibo@i.pkuschool.edu.cn

Purpose: To investigate the effect of alternating-day diet regimens on high-fat diet-induced metabolic disorders in mice.

Materials and Methods: Eight-week-old C57BL/6J mice were fed with either a continuous normal chow diet (CD, n = 10), a continuous high-fat diet (HFD, n = 10), HFD alternating every 24 h with fasting (H-ADF, n = 20), or HFD alternating every 24 h with chow diet (H-ADC, n = 20) for 12 weeks. Weights were recorded weekly and oral glucose tolerance tests were performed 6 weeks after initiating the regimens. At the end of the study, blood samples were collected and serum insulin and lipids were measured; tissues were collected for histology and RNA-seq analysis.

Results: HFD significantly increased body weight and fat percentage, while HFD alternating with fasting or CD did not significantly affect body weight and fat percentage. The glucose intolerance induced by HFD was also significantly ameliorated in these two diet intervention groups. HFD-induced elevation of total cholesterol, low-density lipoprotein and insulin were also reduced in H-ADF and H-ADC groups. Moreover, HFD-disturbed immunity, presented by Lysozyme C-1 (Lyz1) immunostaining and RNA-seq, was restored in both alternating-regimen groups, especially, with H-ADC. At the transcriptional level, some cell proliferation and lipid absorption pathways were down-regulated in both H-ADF and H-ADC groups compared to the continuous HFD group.

Conclusion: Alternating an HFD with a normal diet every 24 h effectively controls weight and prevents metabolic disorders and may act by affecting both fat absorption and intestinal immunity.

Keywords: intermittent fasting, high-fat diet, intestines, obesity, absorption, intestinal immunity

Introduction

Obesity, defined as body mass index (BMI) equal to or greater than 30, is a global public health problem. In 2016, 650 million adults, approximately 13% of the world-wide population, were obese. The health consequences of obesity include type 2 diabetes, cardiovascular diseases, musculoskeletal problems, and cancer, among other conditions (World Health Organization, 2021). Most obesity can be attributed to an imbalance between energy intake and expenditure.^{1,2}

It is well recognized that a high-fat diet (HFD) or a high-fat high-sugar diet causes obesity and related metabolic diseases in rodents, primates, and humans.³⁻⁷ Moreover, overnutrition stimulates intestinal epithelial proliferation and is partially responsible for diet-induced obesity.^{4,8} Caloric restriction, reducing food intake without malnutrition, is an effective regimen for body weight control and has received considerable research attention.⁹⁻¹¹ Recently, intermittent fasting (IF) with alternating dietary regimens was shown to be effective for weight loss in overweight and obese patients¹²⁻¹⁵ and in rodent studies.^{16,17} Among the various IF regimens, alternate-day fasting (ADF) is most frequently studied in rodents and showed profound metabolic benefits through multiple signaling pathways.^{12,17-20} Although previous studies have suggested that it is the gut microbiome most implicated in ADF-induced weight control,^{21,22} one would expect concomitant changes in the small intestine, the primary site of nutrient absorption. However, these

have never been examined, neither functionally nor structurally. Therefore, understanding the changes and mechanisms of how the intestine participates in body weight control under different IF regimens should provide new insights into protection from obesity and related metabolic diseases. In this study, we investigated the morphological and molecular changes of the intestine after HFD alone and HFD alternating with fasting. We also investigated the metabolic phenotypes and intestinal changes of alternating HFD with normal chow diet, which can avoid hunger pangs common on the fasting day and should be more feasible for long-term intervention.

Materials and Methods

Experimental Animal Model

All animal protocols were designed to minimize pain or discomfort to

the animals and approved by the Institutional Animal Care and Use Committee of Peking University (approval No. IMMZhangXQ-7) and conducted according to the principles of laboratory animal care of the National Academy of Sciences/National Research Council. Six-week-old C57BL/6J male mice were purchased from Charles River (Beijing, China). Mice were housed with controlled light (12 h light-dark cycle), temperature (21–23°C) and 45–55% humidity, ad libitum access to chow diet (CD) and water for 2 weeks to acclimate to the new environment before the study was initiated. A high-fat diet (D12492, a rodent diet with 5240 kcal/kg, including 60 kcal% fat, 20 kcal% protein and 20 kcal % carbohydrate, Research Diets, New Brunswick, NJ), and a standard laboratory chow diet (SWS9102, a rodent diet with 3530 kcal/kg, including 12 kcal% fat, 20.6 kcal% protein and 67.4 kcal% carbohydrate, Jiangsu Xietong Pharmaceutical Bio-engineering, Nanjing, China) were used in this study.

At 8 weeks old, mice were randomly divided into continuous chow diet (CD, $n = 10$), continuous high fat diet (HFD, $n = 10$), HFD with alternate-day fasting (H-ADF, $n = 20$) and HFD with alternate-day CD (H-ADC, $n = 20$) group. Both CD and HFD groups were given unrestricted access to food, while the mice in the H-ADF group were alternately provided 24 h of free access to HFD (D12492, Research Diets, New Brunswick, NJ, USA) followed by 24 h of fasting. The H-ADC group of mice was alternately provided 24 h of free access to HFD followed by 24 h of free access to CD (Figure 1A). Body weight was measured once a week, and the body fat ratio was measured a week prior to sacrifice. For both intermittent diet groups, the body weight and body fat ratio were measured on an HFD-feeding day. Body fat ratio was measured using an EchoMRI-100 body composition analyzer (Echo Medical Systems, TX, USA).

Glucose Tolerance Test

An oral glucose tolerance test (oGTT) was conducted 6 weeks after the start of the study. The mice fasted overnight, and glucose intragastric gavage was carried out at 2 g/kg body weight. Blood samples were taken from the tail prior to glucose gavage at 0 (baseline), 15, 30, 60, and 120 minutes post gavage for glucose measurement. For both intermittent diet groups, the overnight fasting was done after an HFD-feeding day. Glucose levels were measured using a glucometer (ACCU-CHEK[®] Performa, Roche, Basel, Switzerland).

Blood Lipids and Serum Insulin Measurement

Serum total cholesterol (TC), triglyceride (TG), low-density lipoprotein (LDL), high-density lipoprotein (HDL) were measured by cobas[®] 4000 analyzer series (Roche, Basel, Switzerland). Insulin levels in serum were measured with an ELISA kit (Mouse Metabolic Hormone Magnetic Bead Panel, Merck Millipore, Billerica, MA, USA).

Lipid Absorption Assay

Mice were fasted for 4 hr and gavaged with BODIPY 500/510 C1, C12 FAs (2 µg/g body weight; #D3823, Molecular Probes Eugene, OR, USA), and olive oil (10 µL/g body weight). The mice were euthanized 2 hr after gavage. The small intestines were excised and embedded in Tissue-Tek O.C.T. Compound (Sakura Finetek, Torrance, CA, USA). Then, 10 µm sections were prepared and mounted with DAPI, and the sections were imaged under a fluorescence microscope.

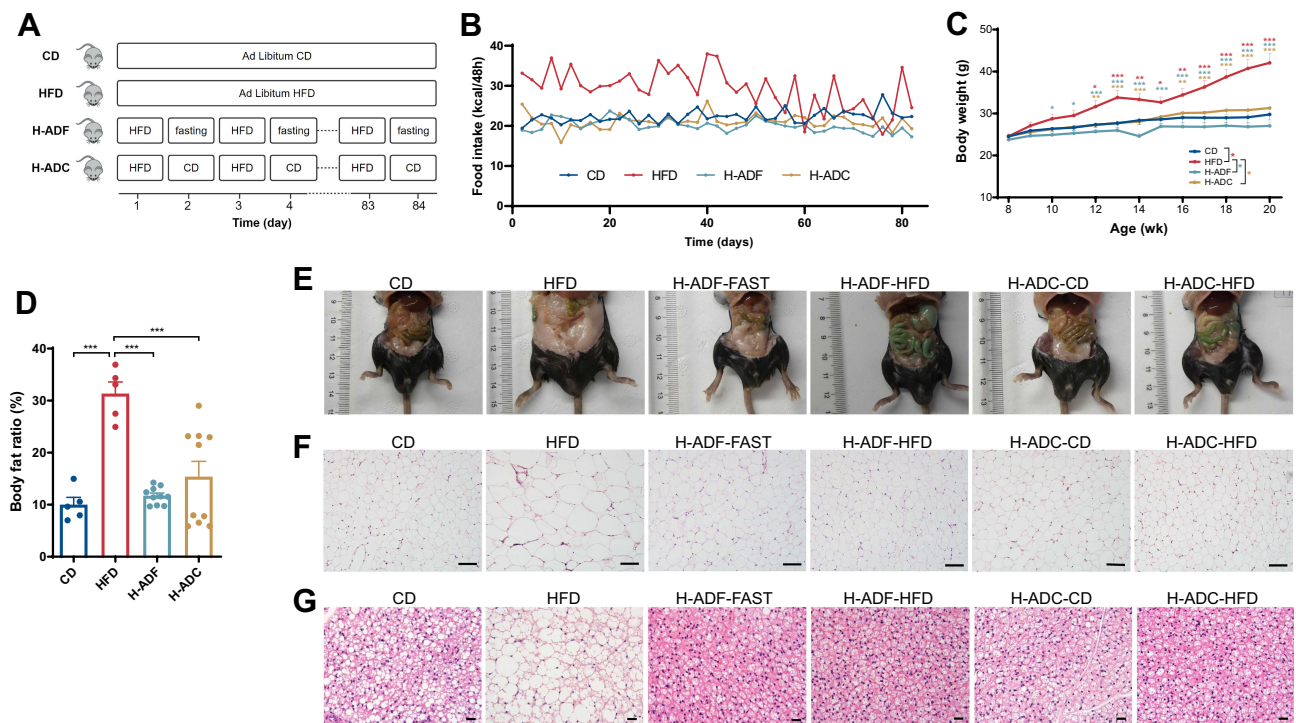


Figure 1 H-ADF and H-ADC ameliorates HFD-induced adiposity. **(A)** Overview of the design of feeding groups. **(B)** Dietary calories for each mouse per 48h. **(C)** Bodyweight ($n = 5$ or 10 per group). Data are presented as mean \pm SE, * $P < 0.05$, ** $P < 0.01$, *** $P < 0.001$. The differences between different feeding groups are compared using two-way ANOVA, repeated-measure, followed by Tukey. **(D)** Body fat ratio ($n = 5$ or 10 per group), *** $P < 0.001$, one-way ANOVA. **(E)** Representative images of body size and intra-abdominal fat. **(F)** Representative images of visceral white adipose tissue (HE-staining), scale bar = $100 \mu\text{m}$. **(G)** Representative images of brown adipose tissue (HE-staining), scale bar = $100 \mu\text{m}$.

Tissue Collection

Half of the H-ADC and H-ADF mice were sacrificed on an HFD diet day (H-ADC-HFD and H-ADF-HFD), and the other half sacrificed on either the CD diet day (H-ADC-CD) or a fasting day (H-ADF-FAST). To evaluate insulin sensitivity, the mice ($n = 3$) were euthanized and the livers were collected 15 min after intraperitoneal injection of insulin (1 U/kg body weight), saline was used as control. Mice were anesthetized prior to the collection of blood samples and then promptly sacrificed by cervical dislocation. To collect different segments of the small intestine, it was removed entirely and rinsed rapidly in ice-cold Ringer's solution (115 mM NaCl , 25 mM NaHCO_3 , 1.2 mM MgCl_2 , 1.2 mM CaCl_2 , $2.4 \text{ mM K}_2\text{HPO}_4$, and $0.4 \text{ mM KH}_2\text{PO}_4$, pH 7.35) supplemented with phenylmethylsulfonyl fluoride. It was then dissected into three parts corresponding to the duodenum, jejunum, and ileum. Abdominal adipose tissue and liver were also collected. All tissue samples were divided into two parts, one part immediately put into liquid nitrogen for RNA or protein extraction, other part immediately fixed in 4% paraformaldehyde (PFA) for further immunohistochemical or histological analysis.

RNA-Seq Analysis

RNA was extracted from intestinal tissues using TRIzol reagent (15596026, Thermo Fisher Scientific, Waltham, MA, USA) in accordance with manufacturer's instructions. Library preparation and RNA-sequencing were conducted by Beijing Genomics Institute (BGI). After library construction, paired-end 150 base pair reads were generated on the DNBseq platform. Differentially expressed genes (DEGs) were analyzed by DESeq2.

Histological Analysis

Tissues fixed in 4% PFA were embedded in paraffin and 3–5 μm sections were prepared. For HE staining, the deparaffinized sections were stained with hematoxylin and eosin solutions, respectively. Oil red O staining was

performed according to the manufacture's instruction (BA4081, BaSO, Zhuhai, China). Briefly, 10 μm liver frozen sections were put into 60% isopropanol for 30s, then stained with oil red O solution for 10 min. Then, the sections were rinsed with 60% isopropanol and phosphate buffer saline (PBS), and subsequently the sections were stained with hematoxylin solution for 1 min. For measurement of length of villi, the HE-stained sections were imaged with a light microscope (BX53, Olympus, Tokyo, Japan). Thirty well-orientated villi per mouse were randomly chosen and measured with Image J.

Lysozyme (Lyz1) Immunofluorescence Staining

For Lyz1 staining, intestinal tissues were fixed in 4% paraformaldehyde. Five-micrometer sections were stained with anti-lyz1 antibody (ZA-0185, ZSGB-BIO, China) overnight at 4 °C, followed by goat anti-rabbit IgG (H+L) cross-adsorbed secondary antibody, Alexa Fluor™ 568 (A-11011, Thermo Fisher Scientific, Waltham, MA, USA) for 1 h at room temperature. The sections were then incubated with DAPI for 20 min at room temperature to label nuclei. The sections were observed under a fluorescence microscopy (BX53, Olympus, Tokyo, Japan), and images were captured by cellSens Standard software (Olympus, Tokyo, Japan). For Paneth cell quantification, intestinal sections from 3 animals were analyzed for each experimental group and at least 30 crypts were counted per animal.

Western Blotting

Liver tissues were homogenized and lysed by RIPA buffer (R0010, Solarbio, China) supplemented with a protease inhibitor cocktail (1:100, Sigma-Aldrich, St. Louis, MO, USA), a phosphatase inhibitor (1:10, Roche, Basel, Switzerland), and 2 mM PMSF. Protein samples were separated by 10% SDS-PAGE and transferred to a PVDF membrane (Merck Millipore, Billerica, MA, USA). The membranes were incubated overnight at 4°C with the following primary antibodies: anti-AKT (1:1000, Cell Signaling Technology, Danvers, MA, USA), anti-p-AKT (Ser473, 1: 1000, Cell Signaling Technology, Danvers, MA, USA), followed by a 1-hr incubation with anti-rabbit horseradish peroxidase-labeled secondary antibodies (1:2000, ZSGB-BIO, China) for 1 hr at room temperature. An ECL detection system (Bio-Rad, Hercules, CA, USA) was used to reveal the peroxidase label. Relative abundance was quantified by densitometry using Image J.

Statistical Analysis

Statistical analysis was performed using one-way or two-way ANOVA with Excel and GraphPad PRISM (Version 8.0, La Jolla, CA, USA). All data are expressed as mean \pm SE. p value <0.05 was considered statistically significant.

Results

H-ADC Has a Similar Effect to H-ADF in Preventing HFD-Induced Adiposity

The calorie consumption in each group was measured daily, and we showed the calorie consumption in every 48 hr to avoid the influence of dietary switch (Figure 1A and B). The body weight of each animal was monitored weekly during the 12-week feeding period. Consistent with previous studies, the H-ADF group displayed a clearly controlled weight increase compared to that of the HFD group and did not show a significant difference in comparison with the CD group. Importantly, the average weekly body weight in the H-ADC group was similar to the CD group (Figure 1C), indicating that like H-ADF, H-ADC feeding is also able to control weight increases usually caused by HFD. In addition, the body fat ratio of the H-ADC group was significantly lower than that of the HFD group and displayed no significant difference when compared to the CD or H-ADF group (Figure 1D). The visceral fat mass was less, and visceral adipocyte size was smaller in both H-ADC and H-ADF groups as compared to the HFD group (Figure 1E and F). In addition, we found that the brown adipocytes in the HFD group were large and filled with lipids, indicating profound brown adipose tissue whitening (Figure 1G). In contrast, the brown fat morphology of mice in both dietary intervention groups was not obviously different from the CD group (Figure 1G). Collectively, these results confirmed that H-ADC feeding could effectively achieve weight control similar to H-ADF.

H-ADC Ameliorates HFD-Induced Metabolic Deterioration

To test glucose metabolism in different feeding groups, oGTT was conducted at 6 weeks after feeding was initiated. Compared to the CD group, the HFD group showed a significantly impaired glucose tolerance, while the glucose curves in H-ADF and H-ADC groups were no different than the CD group (Figure 2A). Consistently, the area under the curve (AUC) of the blood glucose levels of the HFD group was significantly higher than the other three groups, and the AUC of the H-ADC group was comparable to CD (Figure 2B). Furthermore, the insulin levels in H-ADC group on CD diet and in the H-ADF group on both diet days were all significantly lower than the HFD group, while the H-ADC group on HFD diet day was not (Figure 2C). In addition, insulin sensitivity evidenced by Akt phosphorylation (p-Akt) was clearly attenuated in the livers of the HFD group but not affected by HFD in H-ADF and H-ADC groups (Figure 2D).

Obesity is usually coupled with dyslipidemia and fatty liver. The total serum cholesterol (TC), low-density lipoprotein (LDL) and high-density lipoprotein (HDL) levels were significantly elevated in the HFD group but decreased in both dietary intervention groups on both alternate diet days (Figure 2E). However, the triglycerides (TG) were not different between CD and HFD groups but decreased in the H-ADC and H-ADF groups when compared with CD or HFD group (Figure 2E). Interestingly, there were also significant ($p < 0.01$) differences in TC, HDL and insulin levels between the animals in the H-ADC regimen harvested on alternate diet days (Figure 2C and E). Liver steatosis investigated by both HE and oil-red O staining showed that there was a much higher rate of liver steatosis in the HFD feeding group, while H-ADF and H-ADC groups showed nearly no difference from the CD group (Figure 2F). These results indicate that H-ADC feeding can effectively protect mice from metabolic disorders to a similar degree as H-ADF.

H-ADC and H-ADF Alleviate HFD-Induced Lipids Absorption and Paneth Cell Dysfunction

Previous studies have shown that HFD induces villus elongation. Therefore, we investigated the intestinal morphology and found that villi in the HFD group were clearly longer than that in the CD group, while the villi in H-ADC mice were shorter than that of the HFD group and displayed no obvious difference from H-ADF or CD mice (Figure 3A and B). In addition, the lipid absorption in the jejunum was enhanced in HFD group compared to CD group but did not alter clearly

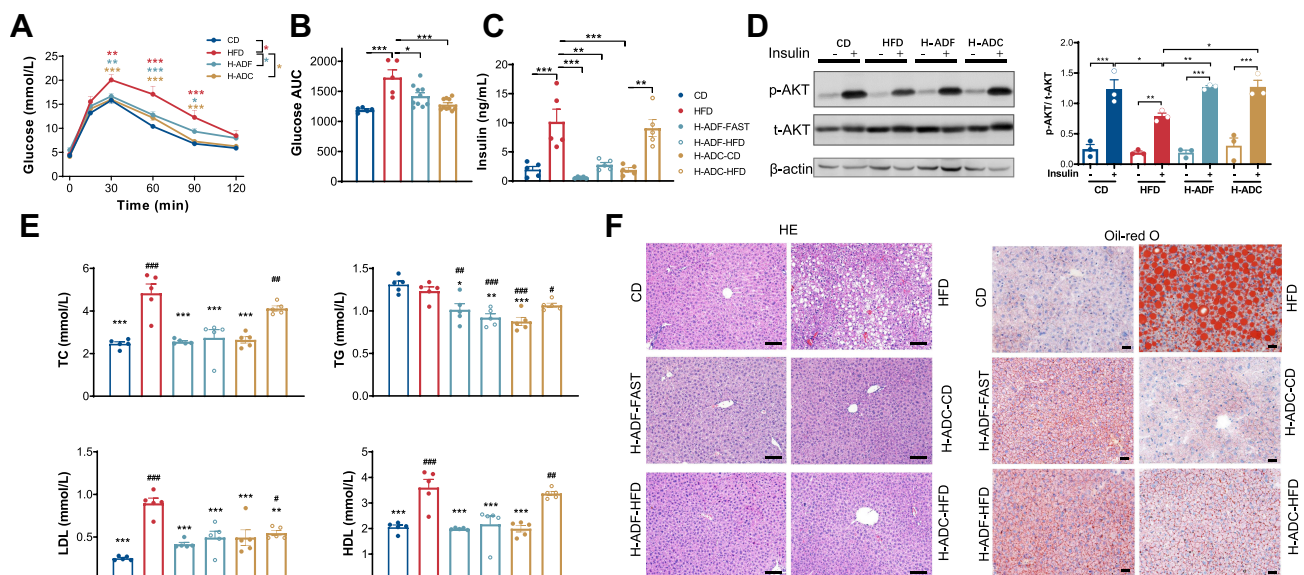


Figure 2 H-ADF and H-ADC ameliorates HFD-induced metabolic disorder. **(A)** Glucose curve of oGTT ($n = 5$ or 10 per group). Data are presented as mean \pm SE, $*P < 0.05$, $**P < 0.01$, $***P < 0.001$. The differences between different feeding groups are compared using two-way ANOVA, repeated-measure, followed by Tukey. **(B)** Area under the curve (AUC) of glucose measured by oGTT. **(C)** Overnight fasting plasma insulin levels ($n = 5$ per group). **(D)** Western blots (left) and statistical analysis (right) of total Akt (t-Akt) and phosphorylated Akt (p-Akt) at ser473 in the liver ($n = 3$ per group). **(E)** Plasma TC, TG, LDL, HDL levels ($n = 5$ per group), $*$ vs HFD, $\#$ vs CD. **(F)** Representative images of liver tissues (HE- and oil red o-staining), scale bar = $100 \mu\text{m}$. Data are presented as mean \pm SE, $*P < 0.05$, $**P < 0.01$, $***P < 0.001$, $\#P < 0.05$, $\#\#P < 0.01$, $\#\#\#P < 0.001$, one-way ANOVA unless otherwise indicated.

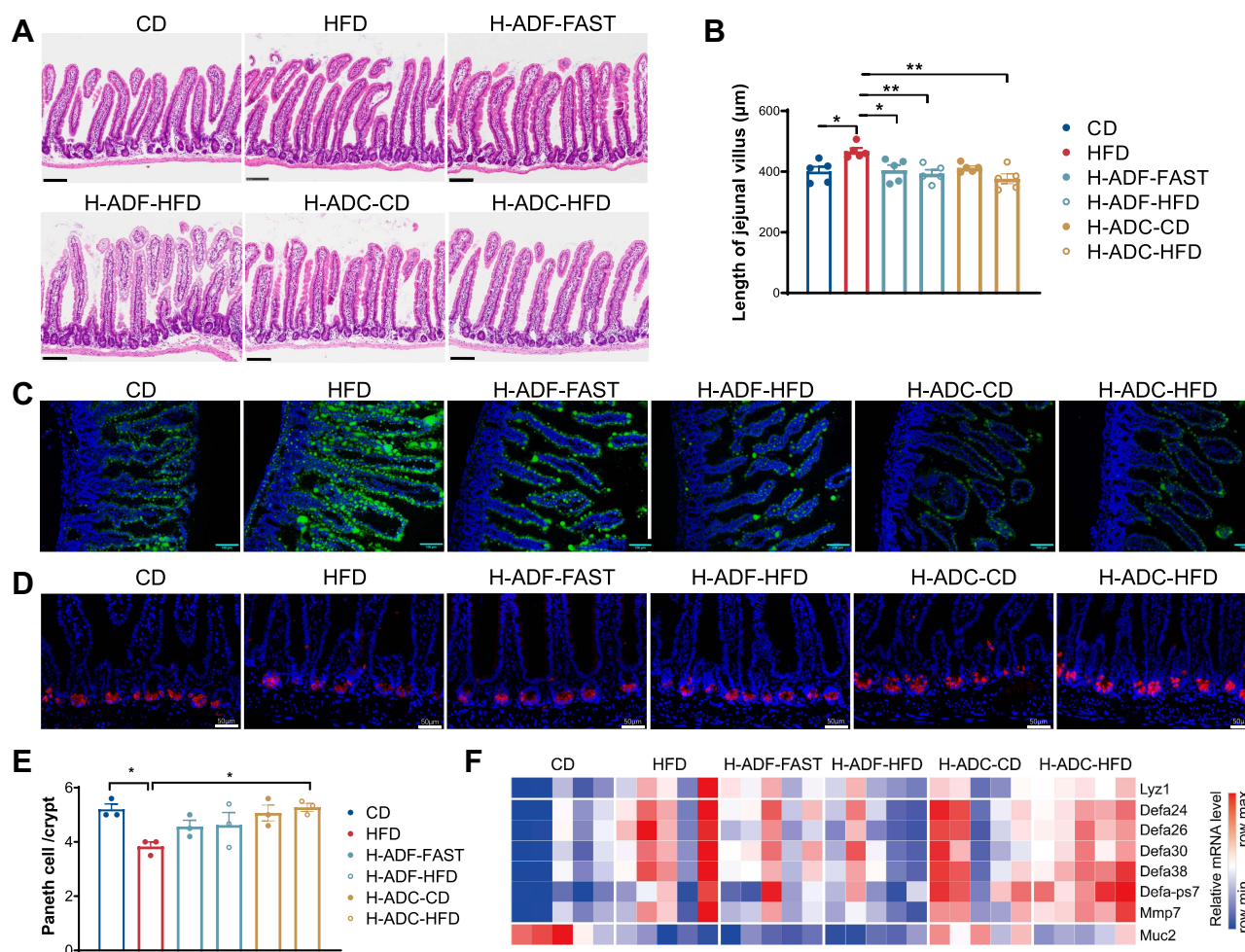


Figure 3 H-ADF and H-ADC prevent HFD-induced lipid absorption and Paneth cell dysfunction. **(A)** Representative images of jejunal tissues (HE-staining), scale bar = 100 μm. **(B)** Length of jejunal villus (n = 5). **(C)** Representative images of the lipid uptake in the jejunum in mice 2 hr after BODIPY-FA gavage. Green fluorescence represents lipids. Scale bar, 100 μm. **(D)** Representative image of Lyz1 immunohistochemistry of jejunum tissues, scale bar = 50 μm. **(E)** Numbers of Paneth cell per crypt (n = 3). **(F)** Heatmap demonstrating the expression of *Lyz1*, α -defensin (*Defa*) family members, *Mmp7* and *Muc2* in the jejunum. Data are presented as mean \pm SE, * P < 0.05, ** P < 0.01, one-way ANOVA.

in H-ADF and H-ADC groups (Figure 3C). Furthermore, we examined the Paneth cells which located in the crypt, and mediate the immune functions in the intestine. HFD-induced Paneth cell dysfunction represented by decreased Lysozyme C-1 (*Lyz1*) immuno-staining was restored in both H-ADC and H-ADF groups (Figure 3D and E), though the mRNA levels of *Lyz1* in both groups were changed similar to the HFD group (Figure 3F), which is consistent with previous reports that HFD reduced Lysozyme C-1 protein expression but induced mRNA expression. In addition, the mRNA levels of many α -defensin family members were also increased in the HFD and two diet intervention groups (Figure 3F). Importantly, HFD-reduced mRNA expression of *Muc2*, a molecule important for intestinal barrier function, was partially ameliorated in the H-ADC group for both diet days, but not in the H-ADF group for both days (Figure 3F). These results suggest that neither H-ADF nor H-ADC feeding has an effect on intestinal morphology, though both H-ADF and H-ADC displayed inhibition of lipid absorption and potential benefits in the protection of Paneth cell dysfunction.

H-ADC-CD Ameliorates HFD-Induced Upregulation of Lipid Metabolism Pathway

For a more comprehensive understanding of the changes in the intestine, we investigated the transcriptome of the jejunum after different diet regimens using RNA-seq analysis. Principal component analysis (PCA) revealed a significant difference in the transcriptional profile between CD and the other three groups in the jejunum (Figure 4A). The transcriptome of the jejunum became distinct from the CD group after HFD, and even though both H-ADF and

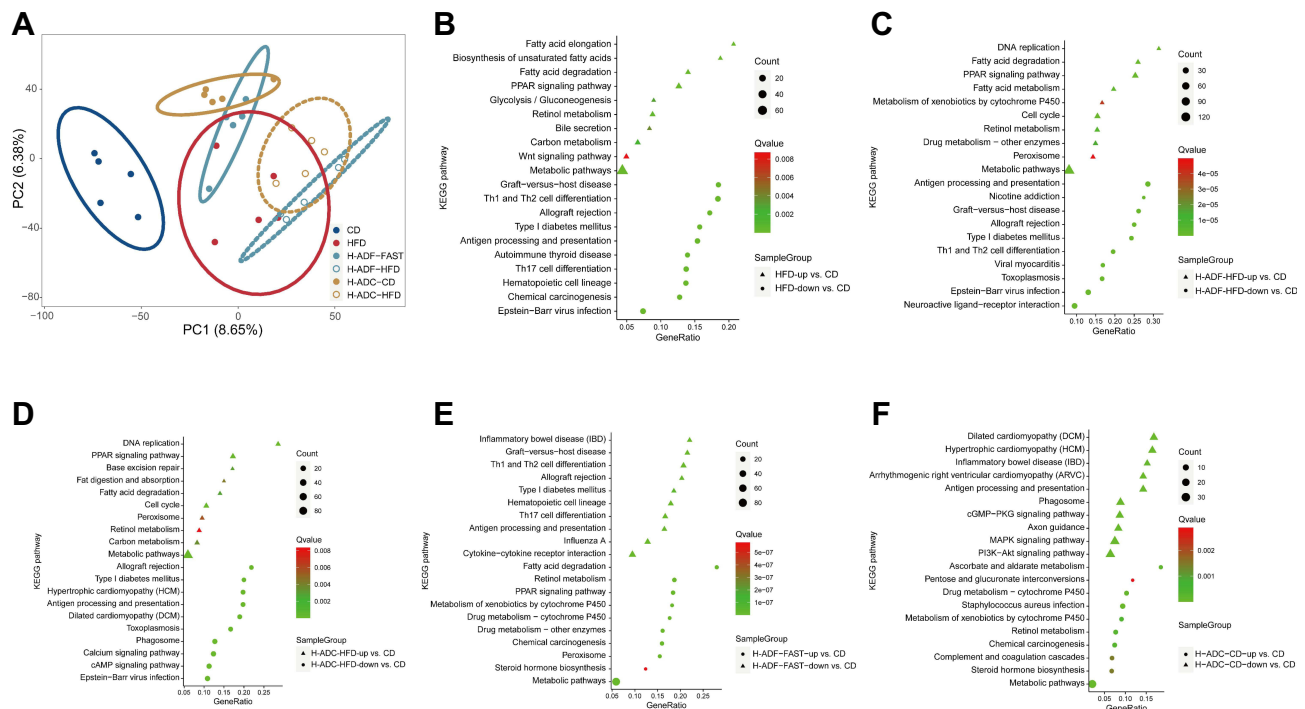


Figure 4 RNA-Seq data analysis. **(A)** PCA score plot of the gene expression data in the jejunum of the 20-wk old mice. **(B–F)** KEGG pathway enrichment analysis of changes in the transcriptome of the jejunum.

H-ADC diets protected mice from obesity and metabolic disorders, their jejunum transcriptomes still differed from that of the CD group (Figure 4A). Both diet intervention groups were close to each other and both partially overlapped with HFD (Figure 4A). Interestingly, the transcriptional profile of H-ADC-CD was separated from both CD and HFD groups, as well as both HFD diet days (H-ADC-HFD and H-ADF-HFD) (Figure 4A). However, the transcriptional profile of the H-ADF-FAST group partially overlapped both the HFD and H-ADC-CD groups (Figure 4A).

Genes upregulated in the HFD, H-ADF group on both HFD and fasting days, and H-ADC at HFD diet day are commonly involved in metabolism-related pathways, especially lipid metabolism pathways, when compared to the CD group (Figure 4B–E), these results are also consistent with the lipid absorption results (Figure 3C). The downregulated genes in the HFD, H-ADF group at both diet days, and H-ADC at HFD diet day are mainly responsible for self-defense and immune functions, as compared to the CD group (Figure 4B–E). However, in H-ADC-CD, the lipid metabolism pathways were not much different from the CD group (Figure 4F).

H-ADC Attenuates HFD-Induced Disturbance of Intestinal Immunity

Next, we analyzed the TPM (Transcripts Per Kilobase Million) of genes from different signaling pathways. Most genes upregulated by HFD in the cell proliferation pathway, which may be responsible for villus elongation, were ameliorated in H-ADC-CD, and some of these genes were also ameliorated in H-ADF-FAST, but not on either HFD diet day (H-ADF-HFD and H-ADC-HFD) (Figure 5A). In the lipid metabolic pathway, some genes involved in fat digestion and absorption upregulated by HFD were reduced in diet intervention groups on fasting or CD diet days, but with no obvious changes with HFD diet days from both diet intervention groups (Figure 5B). Interestingly, we found that negative inhibitors of inflammation and immune response CD200R family members were down-regulated by HFD in the intestine, and the reduction was ameliorated by H-ADC on either HFD or CD diet days, but not by H-ADF either with HFD or fasting (Figure 5C). Furthermore, the killer cell lectin-like receptor (KLR) family molecules, which also function in immune response, were also down-regulated by HFD in the intestine, and the reduction was also ameliorated by H-ADC on either diet day, but they were not restored by H-ADF on either diet day (Figure 5D). These results indicate that HFD enhanced intestinal lipid absorption but impaired intestinal immunity. Thus, H-ADC protected the intestine from HFD-

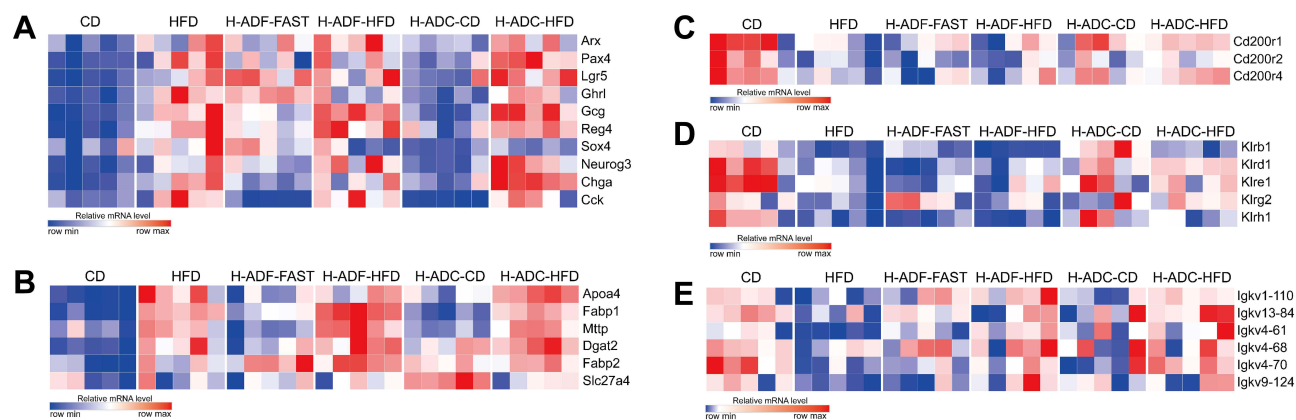


Figure 5 H-ADC suppresses cell proliferation and restores immunity in small intestine. **(A)** Heatmap showing the expression of cell proliferation-related genes. **(B)** heatmap showing the expression of absorption-related genes. **(C–E)** heatmap showing the expression of immunity-related genes.

induced immunity impairment. Interestingly, the expression of many immunoglobulin kappa variable (Igkv) family genes, which have mostly unknown functions and may be related to leukemia, was down-regulated by HFD but alleviated in H-ADF and H-ADC groups (Figure 5E). This suggests one potential common mechanism for both diet interventions in relation to the beneficial effects on weight control and metabolic disorders.

Discussion

Obesity is closely linked to excess intake of energy from food.^{2,23} Recently, intermittent fasting with different dietary patterns showed an effect on weight loss in overweight and obese patients.^{12,14,15} Within that, alternate-day fasting (ADF) is one of the most frequently used diet regimens and has been extensively studied in rodents.^{17–20} However, the hunger pangs on the fasting day are hard to tolerate, making the diet difficult to apply for long-term intervention, so there is an urgent need to have a more suitable regimen for weight control. In addition, changes in the intestine, the main site for nutrient absorption, have not been investigated under ADF. In the current study, we investigated the effects of alternating a high fat diet with a normal chow one (H-ADC) to avoid hunger pangs, as well as alternating a high fat diet with fasting (H-ADF), on weight control and metabolic changes and analyzed the intestinal changes after both H-ADC and H-ADF feeding.

The expression of lipid absorption-related genes in the jejunum of HFD, H-ADF (H-ADF-HFD and H-ADF-FAST), and H-ADC-HFD differed dramatically from CD group, while there was no obvious difference between H-ADC-CD and the CD group. However, the increase in some lipid absorption genes was ameliorated in both diet intervention groups with either CD or fasting. Similar phenomena were also observed for the expression of cell proliferation-related genes. HFD- or high-fat high-sugar diet-induced intestinal epithelial cell proliferation has been suggested to contribute to diet-induced obesity.^{4,8} These results suggest that when high fat is ingested on an HFD diet day, the lipid absorption- and cell proliferation-related gene expression is not affected significantly in the H-ADF and H-ADC groups. However, when the animal switches to CD or fasting, HFD-stimulated lipid absorption- and cell proliferation-related gene expression is reduced, and these changes might slow down intestinal villi elongation and intestinal absorption and may be responsible for the beneficial effects on weight control from both diet intervention groups.

Systemic chronic inflammation has long been suggested to be involved in obesity and related to metabolic disorders.^{24–26} Besides nutrient absorption, the intestine is also an important immune organ, by itself or through interactions with the gut microbiome, and is implicated in the development of many diseases. Intestinal Paneth cells play a critical role in modulating innate immunity and infection.²⁷ It has been reported that obesity is related to Paneth cell dysfunction in man, represented by decreased HD5 and Lysozyme C protein expression, while mRNA levels of *HD5* (*DEFA5*) and *LYZ* are increased.^{28,29} The typical Western diet also induces Paneth cell dysfunction in mice.²⁹ Consistent with these findings, we found that the protein level of Lysozyme C-1 was decreased and the transcription of *Lyz1* was increased with HFD. However, the loss of Lysozyme C-1 protein was prevented in both H-ADC and H-ADF groups,

even though *Lyz1* mRNA expression tended to increase on HFD diet days in H-ADC. This protection for Paneth cells might be partially responsible for the beneficial metabolic effects. Interestingly, many α -defensin family members also showed a similar trend of changes; these changes may further confirm the important role of Paneth cells in diet-induced metabolic disorders. While both H-ADC and H-ADF have similar protective effects on Paneth cells, the underlying mechanisms are not totally the same and need further investigation.

Studies have demonstrated that the immune inhibitory receptor CD200R is implicated in many diseases, and decreased CD200-CD200R signaling is associated with multiple inflammatory diseases and tumor.^{30–33} Here, we found that the expression of CD200R was profoundly reduced in HFD and H-ADF groups but was clearly ameliorated in H-ADC on both HFD and CD diet days. In addition, many killer cell lectin-like receptors (KLR) are also critical for maintaining the immuno-homeostasis and inhibition of inflammation.^{34,35} In our study, the reduction of many KLRs by HFD was also profoundly restored in the H-ADC group, but less in the H-ADF group. Interestingly, we found another possible immune-response family, *Igkv*, which was also reduced by HFD and partially restored by H-ADF or H-ADC. However, the function of this family of immunoglobulins is largely unknown, but the data here demonstrate that they are worthy of further investigation.

The intestinal barrier is important for intestinal functioning and controlling extra-intestinal inflammation. In this study, we found that *Muc2* expression is largely reduced in HFD and H-ADF, but this reduction was partially ameliorated by H-ADC. These results demonstrate that in addition to reducing nutrient absorption, H-ADC restores intestinal immunity and barrier function. This should also contribute to its beneficial effects on metabolic disorders, indicating that H-ADC is a highly suitable diet intervention regimen for weight control.

Taking together, our findings indicate that besides appositional function, intestinal immunity may also be an important contributor of diet-induced obesity and is worthy of further investigation. Finally, there are many other pathways, other than those mentioned, that are up or downregulated by H-ADF or H-ADC, so further studies to investigate these changes may provide additional insights into weight control induced by these diet regimens. However, the mechanisms of dietary interventions, especially the H-ADC diet, on the gut as well as metabolism we discovered in this study have not been reported from clinical studies, which requires further investigation.

Acknowledgments

The authors thank Pamela B. Wright help with editing the English. We also thank Dr. Xiuqin Zhang for providing critical comments and scientific discussion, Ning Hou for their technical support, and Haibao Shang for animal experiments. This work was supported by the National Natural Science Foundation of China (81970690 and 81471063).

Author Contributions

All authors made a significant contribution to the work reported. D.Z.A. and Y.Y. conceived and designed the project, performed experiments, analyzed and interpreted data. W.Z. conceived the project. Y.X. and X.S. performed experiments. All authors took part in drafting, revising or critically reviewing the article; gave final approval of the version to be published; have agreed on the journal to which the article has been submitted; and agree to be accountable for all aspects of the work.

Disclosure

The authors report no potential conflicts of interest relevant to this article.

References

1. Scarborough P, Burg MR, Foster C., et al. Increased energy intake entirely accounts for increase in body weight in women but not in men in the UK between 1986 and 2000. *Br J Nutr.* 2011;105(9):1399–1404. doi:10.1017/S0007114510005076
2. Swinburn B, Sacks G, Ravussin E. Increased food energy supply is more than sufficient to explain the US epidemic of obesity. *Am J Clin Nutr.* 2009;90(6):1453–1456. doi:10.3945/ajcn.2009.28595
3. van der Heijden RA, Sheedfar F, Morrison MC, et al. High-fat diet induced obesity primes inflammation in adipose tissue prior to liver in C57BL/6j mice. *Aging.* 2015;7(4):256–268. doi:10.18632/aging.100738

4. Aliluev A, Tritschler S, Sterr M, et al. Diet-induced alteration of intestinal stem cell function underlies obesity and prediabetes in mice. *Nat Metab.* 2021;3(9):1202–1216. doi:10.1038/s42255-021-00458-9
5. Jimenez-Gomez Y, Mattison JA, Pearson KJ, et al. Resveratrol improves adipose insulin signaling and reduces the inflammatory response in adipose tissue of rhesus monkeys on high-fat, high-sugar diet. *Cell Metab.* 2013;18(4):533–545. doi:10.1016/j.cmet.2013.09.004
6. Zhao Y, Wang L, Xue H, Wang H, Wang Y. Fast food consumption and its associations with obesity and hypertension among children: results from the baseline data of the Childhood Obesity Study in China Mega-cities. *BMC Public Health.* 2017;17(1):933. doi:10.1186/s12889-017-4952-x
7. Monteiro LZ, Varela AR, Lira BA, et al. Weight status, physical activity and eating habits of young adults in Midwest Brazil. *Public Health Nutr.* 2019;22(14):2609–2616. doi:10.1017/S1368980019000995
8. Mao J, Hu X, Xiao Y, et al. Overnutrition stimulates intestinal epithelium proliferation through β -catenin signaling in obese mice. *Diabetes.* 2013;62(11):3736–3746. doi:10.2337/db13-0035
9. Zijlmans DGM, Maaskant A, Louwse AL, Sterck EHM, Langermans JAM. Overweight Management through Mild Caloric Restriction in Multigenerational Long-Tailed Macaque Breeding Groups. *Vet Sci.* 2022;9(6). doi:10.3390/vetsci9060262
10. Yamada Y, Colman RJ, Kemnitz JW, et al. Long-term calorie restriction decreases metabolic cost of movement and prevents decrease of physical activity during aging in rhesus monkeys. *Exp Gerontol.* 2013;48(11):1226–1235. doi:10.1016/j.exger.2013.08.002
11. Colman RJ, Anderson RM, Johnson SC, et al. Caloric restriction delays disease onset and mortality in rhesus monkeys. *Science.* 2009;325(5937):201–204. doi:10.1126/science.1173635
12. de Cabo R, Mattson MP. Effects of intermittent fasting on health, aging, and disease. *N Engl J Med.* 2019;381(26):2541–2551. doi:10.1056/NEJMr1905136
13. Razavi R, Parvaresh A, Abbasi B, et al. The alternate-day fasting diet is a more effective approach than a calorie restriction diet on weight loss and hs-CRP levels. *Int J Vitam Nutr Res.* 2021;91(3–4):242–250. doi:10.1024/0300-9831/a000623
14. Trepanowski JF, Kroeger CM, Barnosky A, et al. Effect of Alternate-Day Fasting on Weight Loss, Weight Maintenance, and Cardioprotection Among Metabolically Healthy Obese Adults: a Randomized Clinical Trial. *JAMA Intern Med.* 2017;177(7):930–938. doi:10.1001/jamainternmed.2017.0936
15. Varady K, Cienfuegos S, Ezpeleta M, Gabel K. Clinical application of intermittent fasting for weight loss: progress and future directions. *Nat Rev Endocrinol.* 2022;18(5):309–321. doi:10.1038/s41574-022-00638-x
16. Wilson RA, Deasy W, Stathis CG, Hayes A, Cooke MB. Intermittent Fasting with or without Exercise Prevents Weight Gain and Improves Lipids in Diet-Induced Obese Mice. *Nutrients.* 2018;10(3):346. doi:10.3390/nu10030346
17. Henderson CG, Turner DL, Swoap SJ. Health Effects of Alternate Day Fasting Versus Pair-Fed Caloric Restriction in Diet-Induced Obese C57Bl/6J Male Mice. *Front Physiol.* 2021;12:641532. doi:10.3389/fphys.2021.641532
18. Zhu S, Surampudi P, Rosharavan B, Chondronikola M. Intermittent fasting as a nutrition approach against obesity and metabolic disease. *Curr Opin Clin Nutr Metab Care.* 2020;23(6):387–394. doi:10.1097/MCO.0000000000000694
19. Joslin PMN, Bell RK, Swoap SJ. Obese mice on a high-fat alternate-day fasting regimen lose weight and improve glucose tolerance. *J Anim Physiol Anim Nutr.* 2017;101(5):1036–1045. doi:10.1111/jpn.12546
20. Liu X, Zhang Y, Ma C, Lin J, Du J. Alternate-day fasting alleviates high fat diet induced non-alcoholic fatty liver disease through controlling PPAR α /Fgf21 signaling. *Mol Biol Rep.* 2022;49(4):3113–3122. doi:10.1007/s11033-022-07142-5
21. Li G, Xie C, Lu S, et al. Intermittent Fasting Promotes White Adipose Browning and Decreases Obesity by Shaping the Gut Microbiota. *Cell Metab.* 2017;26(4):672–685.e674. doi:10.1016/j.cmet.2017.08.019
22. Frank J, Gupta A, Osadchiy V, Mayer EA. Brain-gut-microbiome interactions and intermittent fasting in obesity. *Nutrients.* 2021;13(2):584. doi:10.3390/nu13020584
23. Hall KD, Heymsfield SB, Kemnitz JW, Klein S, Schoeller DA, Speakman JR. Energy balance and its components: implications for body weight regulation. *Am J Clin Nutr.* 2012;95(4):989–994. doi:10.3945/ajcn.112.036350
24. Hotamisligil GS. Inflammation and metabolic disorders. *Nature.* 2006;444(7121):860–867. doi:10.1038/nature05485
25. Sattiel AR, Olefsky JM. Inflammatory mechanisms linking obesity and metabolic disease. *J Clin Invest.* 2017;127(1):1–4. doi:10.1172/JCI92035
26. Nobs SP, Zmora N, Elinav E. Nutrition regulates innate immunity in health and disease. *Annu Rev Nutr.* 2020;40(1):189–219. doi:10.1146/annurev-nutr-120919-094440
27. Adolph TE, Tomczak MF, Niederreiter L, et al. Paneth cells as a site of origin for intestinal inflammation. *Nature.* 2013;503(7475):272–276. doi:10.1038/nature12599
28. Hodin CM, Verdum FJ, Grootjans J, et al. Reduced Paneth cell antimicrobial protein levels correlate with activation of the unfolded protein response in the gut of obese individuals. *J Pathol.* 2011;225(2):276–284. doi:10.1002/path.2917
29. Liu TC, Kern JT, Jain U, et al. Western diet induces Paneth cell defects through microbiome alterations and farnesoid X receptor and type I interferon activation. *Cell Host Microbe.* 2021;29(6):988–1001.e1006. doi:10.1016/j.chom.2021.04.004
30. Casulli J, Fife ME, Houston SA, et al. CD200R deletion promotes a neutrophil niche for Francisella tularensis and increases infectious burden and mortality. *Nat Commun.* 2019;10(1):2121. doi:10.1038/s41467-019-10156-6
31. Gao S, Hao B, Yang XF, Chen WQ. Decreased CD200R expression on monocyte-derived macrophages correlates with Th17/Treg imbalance and disease activity in rheumatoid arthritis patients. *Inflamm Res.* 2014;63(6):441–450. doi:10.1007/s00011-014-0716-6
32. Fraser SD, Sadofsky LR, Kaye PM, Hart SP. Reduced expression of monocyte CD200R is associated with enhanced proinflammatory cytokine production in sarcoidosis. *Sci Rep.* 2016;6:38689. doi:10.1038/srep38689
33. Kotwica-Mojzycz K, Jodłowska-Jędrych B, Mojzycz M. CD200:CD200R Interactions and Their Importance in Immunoregulation. *Int J Mol Sci.* 2021;22(4):1602. doi:10.3390/ijms22041602
34. Robbins SH, Nguyen KB, Takahashi N, Mikayama T, Biron CA, Brossay L. Cutting edge: inhibitory functions of the killer cell lectin-like receptor G1 molecule during the activation of mouse NK cells. *J Immunol.* 2002;168(6):2585–2589. doi:10.4049/jimmunol.168.6.2585
35. Raulet DH, Gasser S, Gowen BG, Deng W, Jung H. Regulation of ligands for the NKG2D activating receptor. *Annu Rev Immunol.* 2013;31:413–441. doi:10.1146/annurev-immunol-032712-095951

Diabetes, Metabolic Syndrome and Obesity: Targets and Therapy

Dovepress

Publish your work in this journal

Diabetes, Metabolic Syndrome and Obesity: Targets and Therapy is an international, peer-reviewed open-access journal committed to the rapid publication of the latest laboratory and clinical findings in the fields of diabetes, metabolic syndrome and obesity research. Original research, review, case reports, hypothesis formation, expert opinion and commentaries are all considered for publication. The manuscript management system is completely online and includes a very quick and fair peer-review system, which is all easy to use. Visit <http://www.dovepress.com/testimonials.php> to read real quotes from published authors.

Submit your manuscript here: <https://www.dovepress.com/diabetes-metabolic-syndrome-and-obesity-targets-and-therapy-journal>